

ADVANCED OPTIMIZATION OF AN LOW-ENERGY ION BEAM DYNAMICS AT LINAC FRONT-END WITH RF FOCUSING

V.S. Dyubkov,*

National Research Nuclear University “MEPhI”, Moscow, Russian Federation

Abstract

A design and development of a linac front-end, that guarantees the required beam, quality is an issue of the day. A linac with RF focusing by means of the accelerating field spatial harmonics is suggested as an alternative to RFQ system. Simulation results of the low-energy proton beam dynamics at linac, that takes into account main linac parameter optimization, based on advanced dynamical acceptance calculation, are presented and discussed.

INTRODUCTION

Projects based on accelerator driven systems are developed in about twenty countries around the world. In order to ensure the safety and stability of this systems it is used well-tried and proven engineering solutions. The initial part of a linear accelerator-driver is a section with spatially homogeneous quadrupole focusing (RFQ), as a general rule. However, a grave drawback of classical RFQ structures is the relatively low acceleration rate that often leads to an increase of the accelerator driver total length. In addition, main losses of the particles typically occur in initial parts of the RFQ sections.

Proton and ion accelerators with RF focusing by means of field spatial harmonics are offered as almost only adequate alternative to the well-proven and reliable RFQ systems for many years [1–3]. Analytical method to control the beam envelope at linac with RF focusing was developed previously to minimize particle losses [4]. The goals of this work are to present results of beam dynamics advanced optimization, which allows one to define main parameters of structure with RF focusing by means of nonsynchronous spatial harmonic which guarantee high acceleration rate under high current transmission.

ANALYTICAL RESULTS

Let's present some results obtained earlier in [4]. One first expresses RF field in an axisymmetric periodic resonant structure as Fourier's representation by spatial harmonics of a standing wave assuming that the structure period is a slowly varying function of a longitudinal coordinate z

$$E_z = \sum_{n=0}^{\infty} E_n I_0(k_n r) \cos\left(\int k_n dz\right) \cos \omega t,$$

$$E_r = \sum_{n=0}^{\infty} E_n I_1(k_n r) \sin\left(\int k_n dz\right) \cos \omega t,$$

where E_n is the n th harmonic amplitude of RF field on the axis; $k_n = (\mu + 2\pi n)/D$ is the propagation wave number for the n th RF field spatial harmonic; μ is the phase advance per D ; D is the resonant structure geometric period; ω is the RF frequency; I_0, I_1 are modified Bessel functions of the first kind.

On averaging over rapid oscillation period one can present the motion equation in the smooth approximation in the following matrix form

$$\ddot{\Upsilon} + \Lambda \dot{\Upsilon} = -L\Phi_{\text{ef}}, \quad (1)$$

where the dot above stands for differentiation with respect to the independent longitudinal coordinate ξ and

$$\Upsilon = \begin{pmatrix} \psi \\ \delta \end{pmatrix}, \quad \Lambda = \begin{pmatrix} 3\kappa & 0 \\ 0 & \kappa \end{pmatrix}, \quad L = \begin{pmatrix} \frac{\partial}{\partial \psi} \\ \frac{\partial}{\partial \delta} \end{pmatrix}.$$

Here $\psi = \tau - \tau^*$ ($\tau = \omega t$, τ^* is a normalized motion time of the reference particle at the laboratory coordinate system), $\xi = 2\pi z/\lambda$, $\delta = 2\pi r/\beta_s \lambda$, $\kappa = \ln'_\xi \beta_s$. Φ_{ef} plays role of an effective potential function (EPF) describing a beam interaction with the polyharmonic field of the system subject to the incoherent particle oscillations.

For example, we consider there are two spatial harmonics at the linac. One of it is the synchronous harmonic with $s = 0$, and another one is the nonsynchronous (focusing) with $n = 1$. In this case one has

$$\begin{aligned} \Phi_{\text{ef}} = & \frac{e_0}{2\beta_s} [I_0(\delta) \sin(\psi + \varphi^*) - \psi \cos \varphi^* - \sin \varphi^*] \\ & + \frac{e_0^2}{64} [I_0^2(\delta) + I_1^2(\delta) - 1] \\ & + \frac{5e_0^2}{256} [I_0^2(3\delta) + I_1^2(3\delta) - 1] \\ & - \frac{e_0^2}{32} [I_0(\delta) \cos \psi - 1] - \frac{5e_0^2}{128} [I_0(3\delta) \cos \psi - 1] \\ & - \frac{e_0 e_1}{32} \{ [I_0(\delta) + I_0(3\delta)] \cos(\psi + 2\varphi^*) - 2 \cos 2\varphi^* \} \\ & + \frac{e_0 e_1}{32} \{ [I_0(\delta) I_0(3\delta) + I_1(\delta) I_1(3\delta)] \cos 2(\psi + \varphi^*) \\ & - \cos 2\varphi^* \}, \end{aligned}$$

where $e_n = e E_n Z \lambda / 2\pi \beta_s^2 m_0 c^2$, φ^* is the reference particle phase.

In order to guarantee effective acceleration under small particle loss it is necessary to optimize a changing of synchronous particle phase & field amplitude so that the Eq. 1 has stable solution for a number of initial conditions.

* vsdyubkov@mephi.ru

NUMERICAL RESULTS

Linac parameters with RF focusing by means of one non-synchronous spatial harmonic were optimized by using numerical self-consistent low-energy proton beam dynamics simulation after beam dynamics optimization in one particle approximation on the basis of obtained analytical results. Self-consistent beam dynamics simulations were performed by using a version of the specialized computer code BEAM-DULAC-ARF based on CIC technique to calculate beam self-space-charge field. Special optimization of the field change law was done & it was based on the supposition that channel acceptance is a nondecreasing function of the longitudinal beam coordinate. Therefore, taking into account the equation of motion for the equilibrium particle, the law of the synchronous harmonic amplitude variation at a field increasing length can be written as

$$\frac{d\widehat{e}_s}{d\xi} = \frac{\widehat{e}_s}{\ell} \frac{d\ell}{d\xi} - \frac{\widehat{e}_s}{\varsigma} \frac{d\varsigma}{d\xi} - \frac{\widehat{e}_s^3 \cos \varphi_s}{\beta_s(0)\widehat{e}_s(0)\varsigma(0)\ell} \varsigma - \frac{\chi \widehat{e}_s^{\frac{9}{2}} \sin 2\varphi_s}{8\beta_s^8(0)\widehat{e}_s^{\frac{3}{2}}(0)\varsigma^{\frac{3}{2}}(0)\ell^{\frac{3}{2}}}, \quad (2)$$

where ς is a longitudinal acceptance phase width; ℓ is a certain function of ξ and it can be found by numerical optimization in every given case, $\widehat{e}_s = e_s \beta_s^2$. χ is the amplitude ratio, that is e_1/e_s . In the accelerating parts of the structures \widehat{e}_s is equal to the constant.

Main linac parameters are listed in Table 1. A variation of the linac parameters are shown in Fig. 1.

Table 1: Basic parameters of linac

Parameter	Value
Operational frequency, MHz	176.1
Total linac length, m	2.0
Bunching length, m	1.7
Input equilibrium particle phase	-90.0°
Output equilibrium particle phase	-25.7°
Input synchronous harmonic amplitude, kV/cm	0.3
Amplitude ratio	7.4
Linac half-aperture, mm	5.0

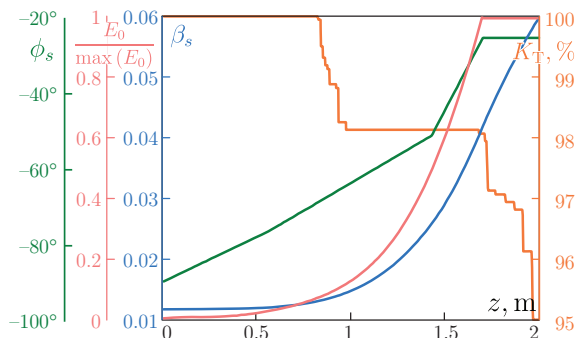


Figure 1: Main linac parameters after optimization.

A calculation of E_0 was performed by using separatrix width calculated for conservative approximation (see curve 1 in Fig. 2) at first. Based on this calculation, particle capture region phase width was found for the non-conservative approximation (curve 2 in Fig. 2). After that, it was used to refine solution of Eq. (2). Finally, numerical simulation was carried out for the found solution above.

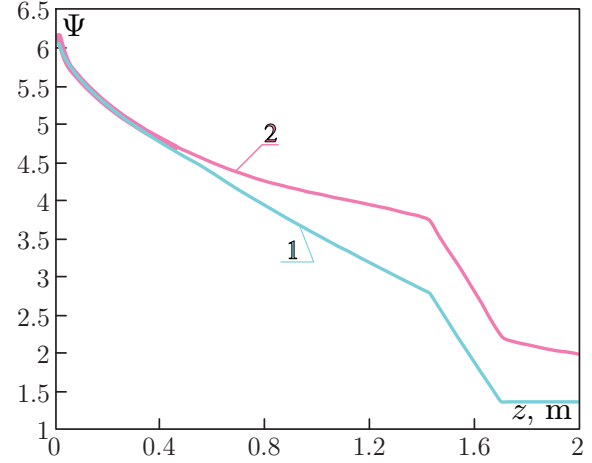


Figure 2: Phase width of longitudinal capture region.

For example, summarized in Table 2 beam parameters were used for computer simulation.

Table 2: Beam parameters @ linac input

Parameter	Value
Particle	p
Input energy, keV	65
Input energy spread, %	1
Input radius, mm	2.5
Input transversal emittance, $\pi \cdot \text{mm} \cdot \text{mrad}$	18
Input beam current, mA	10

Obtained numerical results are presented in Fig. 3-5.

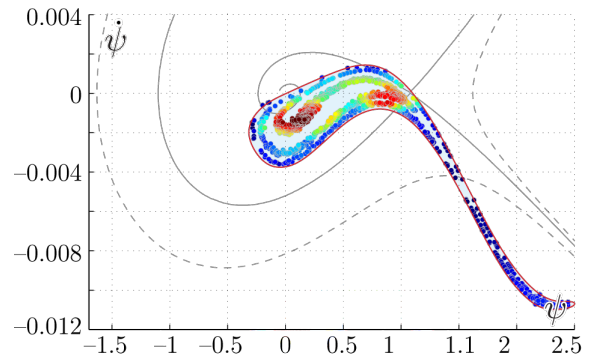


Figure 3: Output longitudinal beam particles distribution.

Output beam energy is equal to 1.7 MeV. Other beam parameters can be estimated by means of presented figures.

Furthermore, halo parameter calculated in accordance with [5] is presented in Fig. 6.

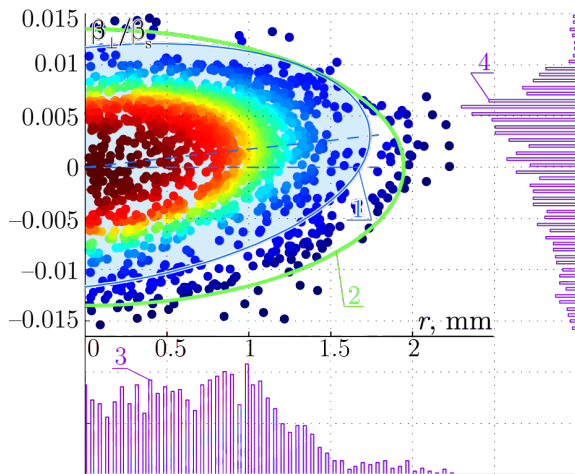


Figure 4: Output transversal beam particles distribution: RMS emittance (1); Floquet ellipse (2); particle distribution by radii (3); particle distribution by β_{\perp} (4).

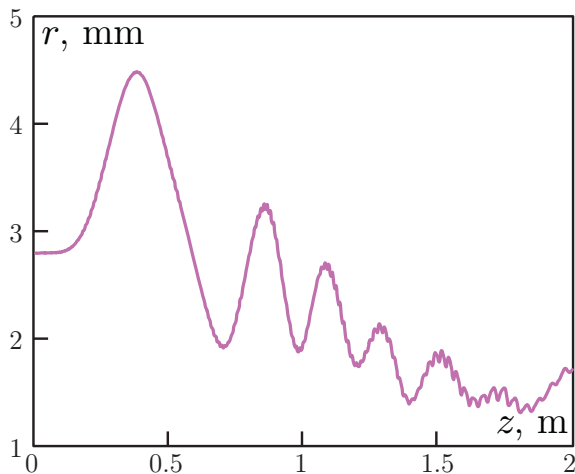


Figure 5: RMS beam radius vs longitudinal coordinate.

Bandwidth of calculated linac channel as a function of injected beam current is shown in Fig. 7.

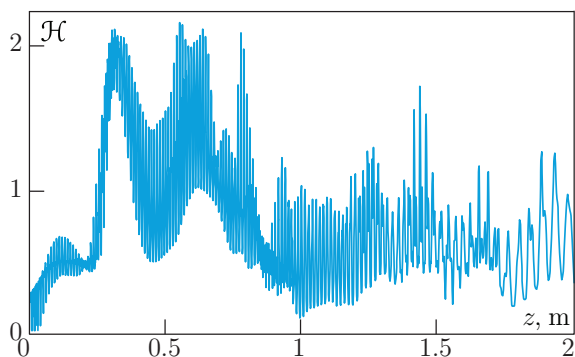


Figure 6: Halo parameter behaviour.

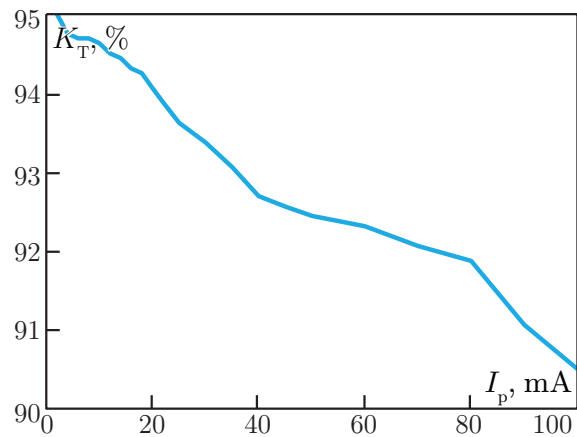


Figure 7: Current transmission vs input beam current.

CONCLUSION

It was shown that advanced optimization allows one to increase current transmission up to 95% under high enough acceleration rate. The main parameters of linac front-end were chosen. There are no beam envelope overgrowth and significant halo formation under chosen parameters at the linac output. Numerical simulation of self-consistent beam dynamics confirmed the analytical results.

REFERENCES

- [1] E.S. Masunov, N.E. Vinogradov, Phys. Rev. ST Accel. Beams 4, 070101 (2001).
- [2] E.S. Masunov et al., "RF focusing methods for heavy ions in low energy accelerators", PAC'03, Portland, May 2003, RPAG035 (2003).
- [3] V.S. Dyubkov, E.S. Masunov, Int. J. Modern Physics A, 24 (5), P. 843 (2009).
- [4] V.S. Dyubkov, S.M. Polozov, "Vestnik of St. Petersburg univ.". Ser. 10: Applied math. Comp. sci. Control proc., 1, P. 135 (2011) (in Russian).
- [5] C.K. Allen, T.P. Wangler, Phys. Rev. ST Accel. Beams 5, 124202 (2002).